Heliyon 10 (2024) e38905

Contents lists available at ScienceDirect

Heliyon

journal homepage: www.cell.com/heliyon

Research article

Molecular modelling and antimicrobial activity of newly synthesized benzothiazolo[3,2-*a*]pyrimidine clubbed thiazole derivatives

Arwa Alharbi [a], Adel I. Alalawy [b], Shaker T. Alsharif [c], Alaa M. Alqahtani [c], Ali H. Alessa [d], Mansoor Alsahag [e], Ali Alisaac [e], Nashwa M. El-Metwaly [a,f,*]

[a] *Department of Chemistry, Faculty of Science, Umm Al-Qura University, Makkah, 24230, Saudi Arabia*
[b] *Department of Biochemistry, Faculty of Science, University of Tabuk, Saudi Arabia*
[c] *Department of Pharmaceutical Chemistry, Faculty of Pharmacy, Umm Al-Qura University, Makkah, 21955, Saudi Arabia*
[d] *Department of Chemistry, Faculty of Science, University of Tabuk, Tabuk, 47512, Saudi Arabia*
[e] *Department of Laboratory Medicine, Faculty of Applied Medical Sciences, Al-Baha University, Saudi Arabia*
[f] *Department of Chemistry, Faculty of Science, Mansoura University, El-Gomhoria Street 35516, Egypt*

ARTICLE INFO

Keywords:
Thiosemicarbazone
Chloroacetone
Benzothiazolopyrimidine-thiazole
DFT
DNA gyrase
SwissADME

ABSTRACT

A series of benzothiazolopyrimidine-thiazole conjugates **7**, **8**, and **9** were produced through the reactions of 8-acetylbenzothiazolopyrimidine-thiosemicarbazone compound **6** with chloroacetone, (un)substituted phenacyl chlorides, and ethyl chloroacetate, respectively. Based on DFT study, the synthesized conjugates had a twisted shape, except for the parent benzothiazolopyrimidine **5** and its thiosemicarbazone compound **6**, which were flat. The study of FMO's also showed that the substituted thiazole derivatives **7** and **8a-c** have equivalent configurations of HOMO and LUMO, as well as exhibiting the least FMO's gap ($\Delta E_{H\text{-}L}$). The antimicrobic activeness of the constructed derivatives has been assessed against the two Gram's types of bacteria and fungi using the broth microdilution method. The benzothiazolopyrimidine-thiazole conjugate **8c** exhibited the strongest inhibition towards Gram-negative *E. coli* (MIC <29 μg/mL), while a valuable performance was observed towards *S. typhimurium* (MIC <132 μg/mL). Also, it displayed broad-spectrum activity with the least MIC *versus C. albicans* fungi (<207 μg/mL). In contrast, the conjugate **8b** demonstrated selective efficacy against Gram + ve *S. aureus* and *B. subtilis* bacteria (MIC <40 and < 47 μg/mL, respectively). Besides, molecular docking of these benzothiazolopyrimidine derivatives with the PDB: 2XCT protein carried out to discover their binding types, RMSD, binding scores, and interactions pocket for each derivative, including a drug reference. Furthermore, their physicochemical-pharmacokinetic profile has estimated *via* the SwissADME prediction. The data indicated that derivative **5** demonstrated constructive pharmacokinetics (M. Wt. 269.28), lipophilicity (Log Po/w = 1.45), and TPSA = 103.47, which foretold high (GI) absorption and good bioavailability = 0.55 without interrupting Lipinski's rules.

* Corresponding author. Department of Chemistry, Faculty of Science, Umm Al-Qura University, Makkah, 24230, Saudi Arabia.
E-mail address: n_elmetwaly00@yahoo.com (N.M. El-Metwaly).

https://doi.org/10.1016/j.heliyon.2024.e38905
Received 16 June 2024; Received in revised form 2 October 2024; Accepted 2 October 2024
Available online 2 October 2024

1. Introduction

Undoubtedly, one of the most serious worldwide health problems is antimicrobial drug resistance (AMR), which has significant implications for disease, death, and economic problems in healthcare classifications across the world [1–5]. The quick progress of multidrug-resistant organisms, known as "superbugs," exposed the effectiveness of current antibiotics and led to diseases that became more problematic to treat [6]. Despite ongoing medical efforts to develop new antibiotics, recent reports indicate that several antibiotics have successfully passed the examination protocol [7–9]. Most of them are analogs of existing compounds, with the potential for stability in original drug enhancement. One interesting choice is to study benzothiazoles, a heterocycle including a 1,3-thiazole ring attached to a benzene ring [10,11]. However, the miscellaneous biological effectiveness of benzothiazoles is determined by their type and position in the drug structure [12–14]. From the previous literature, variations in the second, fifth, and sixth positions of the benzothiazole ring allowed for the synthesis of analogs having a widespread pharmacological properties [15–17]. Besides, several studies have shown that benzothiazole analogs effectively inhibit multiple bacterial pathways, including cell wall synthesis, DNA replication, and essential metabolic processes [14,18–21]. Meanwhile, benzothiazole played a vital role in the enzymatic block concerned with pathogenic bacterial growth, including dihydroorotase, DNA gyrase, and diverse reductases [22]. Given the urgent need to inhibit antimicrobial effectiveness, the creation of benzothiazole derivatives is a probable advance [23]. By targeting available molecular processes, these derivatives may lead to the improvement of novel antimicrobials capable to overcome the strains resistant. On the other hand, pyrimidine analogs play an imperative responsibility in both biochemistry and pharmacology, serving as the base for a wide range of bioactive molecules [24,25]. These pyrimidine candidates are vital models of DNA and RNA because they comprise the pyrimidine bases of cytosine, thymine, and uracil [26]. The ubiquity of these bases in genetic substantial underscores the vital importance of pyrimidine in biological development [27]. In addition to their genetic importance, pyrimidine analogs have a wide spectrum of pharmacological influences, encouraging substantial research into their medical prospective [28]. Meanwhile, several articles confirm their effectiveness in variable applications, as well as their antibacterial, antioxidant, antiviral, anxiolytic, and anticancer effectiveness [29–32]. Pyrimidine analogs also reveal analgesic, anti-inflammatory, and anti-HIV character, representing their role in therapeutic advancement [25,33,34]. The difference in chemical structure of pyrimidine analogs, chiefly those linked to other heterocyclic rings such as thiazolo-pyrimidines, thiano-pyrimidines, and pyrido-pyridines, makes them more useful in medication [35]. Also, substitution by another heterocyclic moieties to the pyrimidine central is a communal method to modify their biological effect and produce pyrimidine analogs with exceptional therapeutic actions [36,37]. Furthermore, thiazolo-pyrimidine analogs are particularly remarkable for their effective antibacterial, anti-inflammatory, and anticancer behaviors [38–40]. Based on previous findings, we expect the current research into benzothiazolo[3,2-*a*]pyrimidine clubbed thiazole derivatives to continue providing key insights and advancements in antimicrobial effectiveness.

2. Experimental

2.1. Instrumental

Melting points of the synthesized conjugates were measured by a Gallenkamp electric device. The IR spectra (KBr discs) were acquired using a ThermoNicolet IS10 FTIR spectrometer. The NMR spectra (^{1}H at 500 MHz and ^{13}C 125 MHz) were obtained in DMSO-d_6 using a JEOL spectrometer. The mass analyses were acquired using a ThermoScientific GC-MS DSQII instrument (70 eV). The elemental constituents C, H, and N were determined by a PerkinElmer 2400 CHN analyzer.

2.2. Synthesis of 6-acetyl-2-(2-cyanoacetamido)benzothiazole (3)

The compound 6-acetyl-2-aminobenzothiazole (**1**) (2.88 g, 15 mmol) and 1-(2-cyanoacetyl)-3,5-dimethyl-1*H*-pyrazole (**2**) (2.44 g, 15 mmol) were mixed together in toluene (35 mL) and then refluxed for 4 h in a 150-mL RB-Flask. The mixture was cooled to 20–25 °C and the obtained solid was separated by filtration and then crystallized by ethanol.

Yield = 81.8 %, m.p. = 221–222 °C. IR (ν/cm^{-1}): 3227 (N-H), 2213 (C ≡ N), 1704, 1675 (C=O). ^{1}H NMR (δ/ppm): 2.56 (s, 3H, $COCH_3$), 3.58 (s, 2H, -CH_2CN), 7.65 (d, J = 8.50 Hz, 1H, benzothiazolyl-H_4), 7.78 (d, J = 8.50 Hz, 1H, benzothiazolyl-H_5), 8.37 (s, 1H, benzothiazolyl-H_7), 11.73 (s, 1H, N-H). Mass analysis, m/z: M^+ = 259 (56.14 %). Analysis for $C_{12}H_9N_3O_2S$ (259.04): Calculated: C, 55.59; H, 3.50; N, 16.21 %. Found: C, 55.71; H, 3.55; N, 16.30 %.

2.3. Synthesis of N-(6-acetylbenzothiazol-2-yl)-2-cyano-3-(dimethylamino)acrylamide (4)

A solution of 6-acetyl-2-(2-cyanoacetamido)benzothiazole (**3**) (2.07 g, 8 mmol) in 30 mL of dioxane was prepared. To this solution, dimethylformamide-dimethylacetal (0.95 mL, 8 mmol) was added in a 100-mL RBF. The solution was subjected to reflux for a period of 4 h and then chilled. The material was filtered and underwent crystallization from ethanol to provide the *N*-benzothiazolyl-3-(dimethylamino)acrylamide compound **4**.

Yield = 60.5 %, m.p. = 253–254 °C. IR (ν/cm^{-1}): 3178 (N-H), 2191 (C ≡ N), 1681, 1658 (C=O). ^{1}H NMR (δ/ppm): 2.54 (s, 3H, $COCH_3$), 3.18 (s, 3H) and 3.31 (s, 3H) [-N(CH_3)$_2$], 7.63 (d, J = 8.50 Hz, 1H, benzothiazolyl-H_4), 7.78 (d, J = 8.50 Hz, 1H, benzothiazolyl-H_5), 7.90 (s, 1H, N-CH=C), 8.38 (s, 1H, benzothiazolyl-H_7), 12.08 (s, 1H, N-H). Mass analysis, m/z: M^+ = 314 (18.56 %). Analysis for $C_{15}H_{14}N_4O_2S$ (314.08): Calculated: C, 57.31; H, 4.49; N, 17.82 %. Found: C, 57.46; H, 4.41; N, 17.71 %.

2.4. Synthesis of 8-acetyl-3-cyano-2-oxo-2H-benzo[4,5]thiazolo[3,2-a]pyrimidine (5)

The *N*-benzothiazolyl-3-(dimethylamino)acrylamide compound **4** (1.25 g, 4 mmol) was suspended in a solution of 20 mL glacial acetic acid. The mixture was then refluxed for a duration of 2 h. The solid that produced upon addition of 20 mL cold water to the solution was then collected using filtering. The crude solid was recrystallized using dioxane as the solvent.

Yield = 83.4 %, m.p. = 285–286 °C. IR (ν/cm^{-1}): 2218 (C ≡ N), 1678, 1654 (C=O). ^{1}H NMR (δ/ppm): 2.54 (s, 3H, $COCH_3$), 6.71 (d, J = 8.50 Hz, 1H, benzothiazolyl-H_4), 7.47 (d, J = 8.50 Hz, 1H, benzothiazolyl-H_5), 7.58 (s, 1H, benzothiazolyl-H_7), 8.64 (s, 1H, pyrimidine-H). ^{13}C NMR (δ/ppm): 27.02, 92.36, 114.60, 115.58, 122.09, 124.74, 126.67, 131.31, 146.45, 158.83, 160.14, 161.93, 197.11. Mass analysis, *m/z*: M^+ = 269 (46.08 %). Analysis for $C_{13}H_7N_3O_2S$ (269.03): Calculated: C, 57.99; H, 2.62; N, 15.61 %. Found: C, 57.87; H, 2.55; N, 15.51 %.

2.5. Synthesis of 2-(1-(3-cyano-2-oxo-2H-benzo[4,5]thiazolo[3,2-a]pyrimidin-8-yl)ethylidene) hydrazine-1-carbothioamide (6)

The 8-acetylbenzothiazolo[3,2-*a*]pyrimidine compound **5** (0.81 g, 3 mmol) was dissolved in 30 mL of ethanol in a 100-mL RBF. Next, thiosemicarbazide (0.27 g, 3 mmol) and 0.5 mL concentrated hydrochloric acid were added to the flask. The mixture was refluxed for a duration of 4 h and thereafter allowed to cool. The powder was separated by filtration to yield the corresponding thiosemicarbazone compound **6**.

Yield = 67.5 %, m.p. = 237–238 °C. IR (ν/cm^{-1}): 3361, 3256, 3178 (-NH_2 and N-H), 2221 (C ≡ N), 1655 (C=O). ^{1}H NMR (δ/ppm): 2.37 (s, 3H, N=C-CH_3), 6.93 (d, J = 8.50 Hz, 1H, benzothiazolyl-H_4), 7.34 (d, J = 8.50 Hz, 1H, benzothiazolyl-H_5), 7.45 (s, 1H, benzothiazolyl-H_7), 7.88 (s, 2H, NH_2), 8.60 (s, 1H, pyrimidine-H), 11.14 (s, 1H, N-H). ^{13}C NMR (δ/ppm): 16.96, 92.43, 115.51, 117.15, 123.55, 124.46, 126.84, 127.63, 144.38, 146.70, 159.01, 160.26, 162.07, 181.11. Mass analysis, *m/z*: M^+ = 342 (32.66 %). Analysis for $C_{14}H_{10}N_6OS_2$ (342.04): Calculated: C, 49.11; H, 2.94; N, 24.55 %. Found: C, 49.32; H, 3.04; N, 24.41 %.

2.6. Synthesis of 3-cyano-8-(1-(2-(thiazol-2-yl)hydrazineylidene)ethyl)-2-oxo-2H-benzo[4,5] thiazolo[3,2-a]pyrimidine derivatives 7 and 8a-c

The thiosemicarbazone compound **6** (0.68 g, 2 mmol) was dissolved in 30 mL of ethanol and triethylamine (0.1 mL). Then, the targeting α-chloroketone (chloroacetone and/or phenacyl chloride derivatives) (2 mmol) was introduced to the solution. The mixture was subjected to reflux for a duration of 4 h and thereafter cooled to a temperature of 25 °C. The isolated product in each instance was subjected to filtration and washed with ethanol to yield the corresponding benzothiazolo[3,2-*a*]pyrimidine-thiazole conjugates **7**, **8a**, **8b**, and **8c**, respectively.

3-Cyano-8-(1-(2-(4-methylthiazol-2-yl)hydrazineylidene)ethyl)-2-oxo-2H-benzo[4,5]thiazolo [3,2-a]pyrimidine (**7**):

Yield = 67.5 %, m.p. = 287–288 °C. IR (ν/cm^{-1}): 3274 (N-H), 2223 (C ≡ N), 1654 (C=O). ^{1}H NMR (δ/ppm): 2.17 (s, 3H, thiazole-CH_3), 2.76 (s, 3H, N=C-CH_3), 6.18 (s, 1H, thiazole-H5), 7.01 (d, J = 8.50 Hz, 1H, benzothiazolyl-H_4), 7.56 (d, J = 8.50 Hz, 1H, benzothiazolyl-H_5), 7.71 (s, 1H, benzothiazolyl-H_7), 8.67 (s, 1H, pyrimidine-H), 11.81 (s, 1H, N-H). ^{13}C NMR (δ/ppm): 16.29, 16.87, 92.37, 104.67, 115.54, 117.04, 123.48, 124.35, 126.95, 127.70, 144.62, 147.04, 158.31, 159.22, 160.41, 161.98, 166.19. Mass analysis, *m/z*: M^+ = 380 (30.27 %). Analysis for $C_{17}H_{12}N_6OS_2$ (380.05): Calculated: C, 53.67; H, 3.18; N, 22.09 %. Found: C, 53.50; H, 3.11; N, 22.21 %.

3-Cyano-2-oxo-8-(1-(2-(4-phenylthiazol-2-yl)hydrazineylidene)ethyl)-2H-benzo[4,5]thiazolo [3,2-a]pyrimidine (**8a**):

Yield = 70.5 %, m.p. = 264–265 °C. IR (ν/cm^{-1}): 3267 (N-H), 2220 (C ≡ N), 1656 (C=O). ^{1}H NMR (δ/ppm): 2.74 (s, 3H, N=C-CH_3), 6.98 (d, J = 8.50 Hz, 1H, benzothiazolyl-H_4), 7.10 (s, 1H, thiazole-H5), 7.33–7.51 (m, 5H, phenyl-H), 7.62 (d, J = 8.50 Hz, 1H, benzothiazolyl-H_5), 7.74 (s, 1H, benzothiazolyl-H_7), 8.68 (s, 1H, pyrimidine-H), 11.76 (s, 1H, N-H). ^{13}C NMR (δ/ppm): 16.74, 92.55, 107.17, 115.46, 117.13, 123.20, 124.31, 126.58, 127.22 (2C), 127.72, 128.63, 129.35 (2C), 133.51, 144.91, 147.69, 158.02, 159.28, 160.34, 161.77, 169.43. Mass analysis, *m/z*: M^+ = 442 (37.44 %). Analysis for $C_{22}H_{14}N_6OS_2$ (442.07): Calculated: C, 59.71; H, 3.19; N, 18.99 %. Found: C, 59.94; H, 3.08; N, 18.83 %.

3-Cyano-8-(1-(2-(4-(4-methoxyphenyl)thiazol-2-yl)hydrazineylidene)ethyl)-2-oxo-2H-benzo [4,5]thiazolo[3,2-a]pyrimidine (**8b**):

Yield = 73.2 %, m.p. = 296–297 °C. IR (ν/cm^{-1}): 3260 (N-H), 2218 (C ≡ N), 1652 (C=O). ^{1}H NMR (δ/ppm): 2.70 (s, 3H, N=C-CH_3), 3.81 (s, 3H, OCH_3), 6.94 (d, J = 8.50 Hz, 2H, phenylene-H), 7.01 (d, J = 8.50 Hz, 1H, benzothiazolyl-H_4), 7.14 (s, 1H, thiazole-H5), 7.55 (d, J = 8.50 Hz, 2H, phenylene-H), 7.63 (d, J = 8.50 Hz, 1H, benzothiazolyl-H_5), 7.74 (s, 1H, benzothiazolyl-H_7), 8.67 (s, 1H, pyrimidine-H), 11.58 (s, 1H, N-H). ^{13}C NMR (δ/ppm): 16.77, 59.81, 92.48, 106.84, 114.96 (2C), 115.41, 117.18, 123.11, 124.23, 125.44, 126.63, 127.70, 128.59 (2C), 144.67, 147.47, 157.91, 159.36, 160.02, 160.29, 161.85, 169.31. Mass analysis, *m/z*: M^+ = 472 (43.02 %). Analysis for $C_{23}H_{16}N_6O_2S_2$ (472.08): Calculated: C, 58.46; H, 3.41; N, 17.79 %. Found: C, 58.59; H, 3.46; N, 17.88 %.

3-Cyano-8-(1-(2-(4-(4-chlorophenyl)thiazol-2-yl)hydrazineylidene)ethyl)-2-oxo-2H-benzo [4,5]thiazolo[3,2-a]pyrimidine (**8c**):

Yield = 64.8 %, m.p. > 320 °C. IR (ν/cm^{-1}): 3278 (N-H), 2221 (C ≡ N), 1656 (C=O). ^{1}H NMR (δ/ppm): 2.78 (s, 3H, N=C-CH_3), 7.03 (d, J = 8.50 Hz, 1H, benzothiazolyl-H_4), 7.17 (s, 1H, thiazole-H5), 7.48 (d, J = 8.50 Hz, 2H, phenylene-H), 7.62 (d, J = 8.50 Hz, 1H, benzothiazolyl-H_5), 7.74 (s, 1H, benzothiazolyl-H_7), 7.85 (d, J = 8.50 Hz, 2H, phenylene-H), 8.70 (s, 1H, pyrimidine-H), 12.01 (s, 1H, N-H). ^{13}C NMR (δ/ppm): 16.70, 92.71, 108.06, 115.53, 117.21, 123.25, 124.38, 126.44, 127.56, 128.78 (2C), 129.52 (2C), 132.30, 134.10, 144.98, 147.84, 158.26, 159.17, 160.30, 161.85, 169.75. Mass analysis, *m/z*: M^+ = 476 (23.19 %). Analysis for $C_{22}H_{13}ClN_6OS_2$ (476.03): Calculated: C, 55.40; H, 2.75; N, 17.62 %. Found: C, 55.24; H, 2.68; N, 17.75 %.

2.7. Synthesis of 3-cyano-2-oxo-8-(1-(2-(4-oxo-4,5-dihydrothiazol-2-yl)hydrazineylidene) ethyl)-2H-benzo[4,5]thiazolo[3,2-a] pyrimidine (9)

Ethyl chloroacetate (0.25 g, 2 mmol) was subjected to reflux with an ethanolic solution (30 mL) of thiosemicarbazone compound **6** (0.68 g, 2 mmol) and fused sodium acetate (0.50 g) for a duration of 4 h. The formed solid upon dilution with cold water (30 mL) was separated by filtration and then subjected to crystallization using dioxane. This process resulted in the desired benzothiazolo[3,2-a] pyrimidine-thiazole conjugate **9**.

Yield = 77.2 %, m.p. = 304–305 °C. IR (ν/cm^{-1}): 3283 (N-H), 2221 (C ≡ N), 1708, 1654 (C=O). ^{1}H NMR (δ/ppm): 2.36 (s, 3H, N=C-CH_3), 4.04 (s, 2H, thiazolidinone-CH_2), 7.01 (d, J = 8.50 Hz, 1H, benzothiazolyl-H_4), 7.58 (d, J = 8.50 Hz, 1H, benzothiazolyl-H_5), 7.71 (s, 1H, benzothiazolyl-H_7), 8.73 (s, 1H, pyrimidine-H), 11.22 (s, 1H, N-H). ^{13}C NMR (δ/ppm): 16.75, 35.79, 92.64, 115.57, 117.20, 123.33, 124.46, 126.61, 127.93, 145.17, 148.14, 159.35, 160.43, 162.03, 163.82, 174.96. Mass analysis, m/z: M^+ = 382 (17.39 %). Analysis for $C_{16}H_{10}N_6O_2S_2$ (382.03): Calculated: C, 50.25; H, 2.64; N, 21.98 %. Found: C, 50.11; H, 2.58; N, 22.10 %.

2.8. DFT modelling

Applying the B3LYP/6–311^{++}G(d,p) procedure comprised in the Gaussian 09W [41–44], the isolated hybrids have been subjected for geometrical optimization, and its electronic and frontier molecular orbitals (FMO's) have been discovered by GaussView [45]. To estimate Fukui indices [46], the DMol3 in Materials Studio's was manipulated at B3LYP/DNP 3.5 [47].

2.9. Antimicrobial assay

The antimicrobial efficacy of the isolated benzothiazolo[3,2-a]pyrimidine clubbed thiazole derivatives towards selected pathogens, such as *Staphylococcus aureus* (*S. aureus*), *Bacillus subtilis* (*B. subtilis*), *Salmonella typhimurium* (*S. typhimurium*), *Escherichia coli* (*E. coli*), and *Candida albicans* (*C. albicans*), was measured using the MIC technique, with Chloramphenicol, Cephalothin, and Cycloheximide as standards, respectively [48–50].

2.10. DNA gyrase

Since DNA gyrase is considered a decisive key in bacterial functions, antibacterial drugs established to treat *E. coli* poisons place a high priority on it. Hindering DNA gyrase activity may result in cells problematic in achieving essential processes, e.g. chromosomal segregation, transcription, and DNA replication. In current work, seven benzothiazolo[3,2-a]pyrimidine clubbed thiazole derivatives towards Ciprofloxacin (Cipro.) standard reference were examined for their inhibition of *E. coli* DNA [51]. However, Ciprofloxacin is a fluoroquinolone antibiotic that operates by inhibiting the replication of bacterial DNA. It is a broad-spectrum antibiotic.

2.11. Molecular docking

The theoretical molecular docking calculation of the synthesized benzothiazolo[3,2-a]pyrimidine clubbed thiazole derivatives was pragmatic for the PDB: 2XCT protein [52]. Meanwhile, re-docking of the co-crystallized ligand (Ciprofloxacin) with DNA gyrase enzyme is performed for validation to inspect the molecular mechanism of the antibacterial effectiveness of the target derivatives [53–55]. Sighting by M.O.E. 2019 program to estimate the suggested binding fashion, affinity, favored alignment of every docking position, and binding energy (S) of the derivatives and co-crystallized DNA gyrase ligand represented by 2XCT protein in contrast to

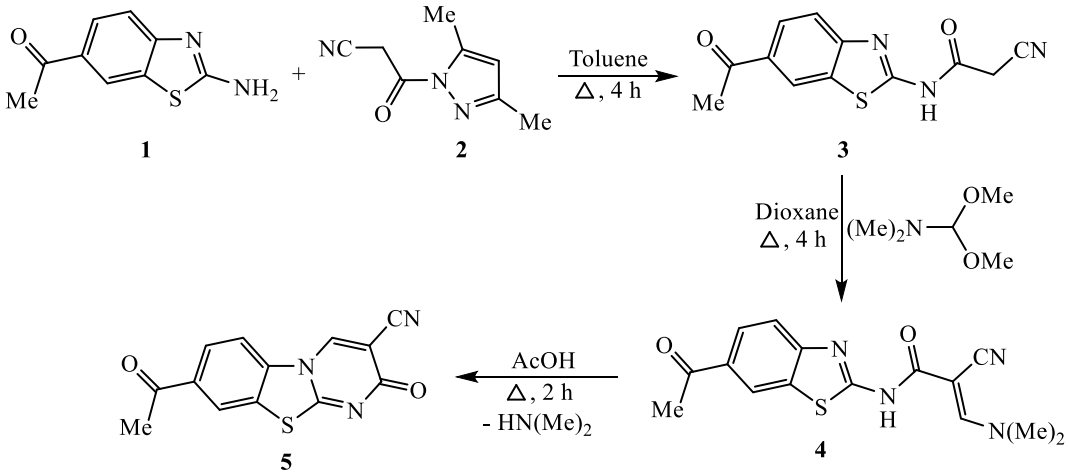

Scheme 1. Synthesis of benzothiazolo[3,2-*a*]pyrimidine compound **5**.

Ciprofloxacin (Cipro). The designed binding energies for the synthesized derivatives correspond to the experimental results by eliminating water and heteroatoms and minimizing the energy with an RMSD lower than two and ten poses.

2.12. SwissADME

The produced derivatives properties were estimated by the SwissADME software from the Swiss Institute of Bioinformatics (www.swissadme.ch). The software integrates Chem Axon's Marvin JS, a molecular sketcher, into its web server, facilitating the creation and modification of 2D chemical structures. SMILES defines the inputs for these structures, listing them on the right side of the submission page for computation. To facilitate export and output, we present the results in an Excel spreadsheet, tables, and graphs, with one panel per molecule.

3. Results and discussion

3.1. Synthesis of benzothiazolopyrimidine-thiazole conjugates 7, 8, and 9

The synthetic pathway for the bifunctional key, 6-acetyl-2-(2-cyanoacetamido)benzothiazole (**3**) was described in Scheme 1. This route involves cyanoacetylation of 6-acetyl-2-aminobenzothiazole (**1**) when treated with 1-(2-cyanoacetyl)-3,5-dimethyl-1*H*-pyrazole (**2**) in boiling toluene. The reactivity of methylene group in the bifunctional key **3** was the motivation to perform the condensation with dimethylformamide-dimethylacetal to afford the corresponding enamine compound, *N*-(6-acetylbenzothiazol-2-yl)-2-cyano-3-(dimethylamino)acrylamide (**4**) as a sole product. The enamine compound **4** undergoes intramolecular elimination of a dimethylamine molecule when heated in acetic acid. This reaction produces the fused tricyclic compound, 8-acetyl-3-cyano-2-oxo-2*H*-benzothiazolo [3,2-*a*]pyrimidine (**5**). The proposed structure was confirmed based on the data of IR, NMR, and mass analyses. The IR spectrum clearly indicated the absorption frequency of nitrile group (C ≡ N) at 2218 cm^{-1}, in addition to the absorption frequencies of two carbonyl functions at 1678 (acetyl) and 1654 cm^{-1} (cyclic). The ^1H NMR signals were identified as a singlet at δ 2.53 ppm for three protons of methyl group ($COCH_3$), doublet for a proton at δ 6.71 ppm (benzothiazolyl-H_4), doublet for a proton at δ 7.47 ppm (benzothiazolyle-H_5), singlet at δ 7.58 ppm for a proton (benzothiazolyl-H_7), and singlet for a proton at δ 8.64 ppm (pyrimidine-H).

The acetyl group located at the eighth position of benzothiazolopyrimidine compound **5** was used to introduce different thiazole ring systems. This resulted in the creation of benzothiazolo[3,2-*a*]pyrimidine-thiazole conjugates **7**, **8**, and **9**. The synthetic strategy was started by the treatment of 8-acetylbenzothiazolo[3,2-*a*]pyrimidine compound **5** with thiosemicarbazide in ethanol and HCl to

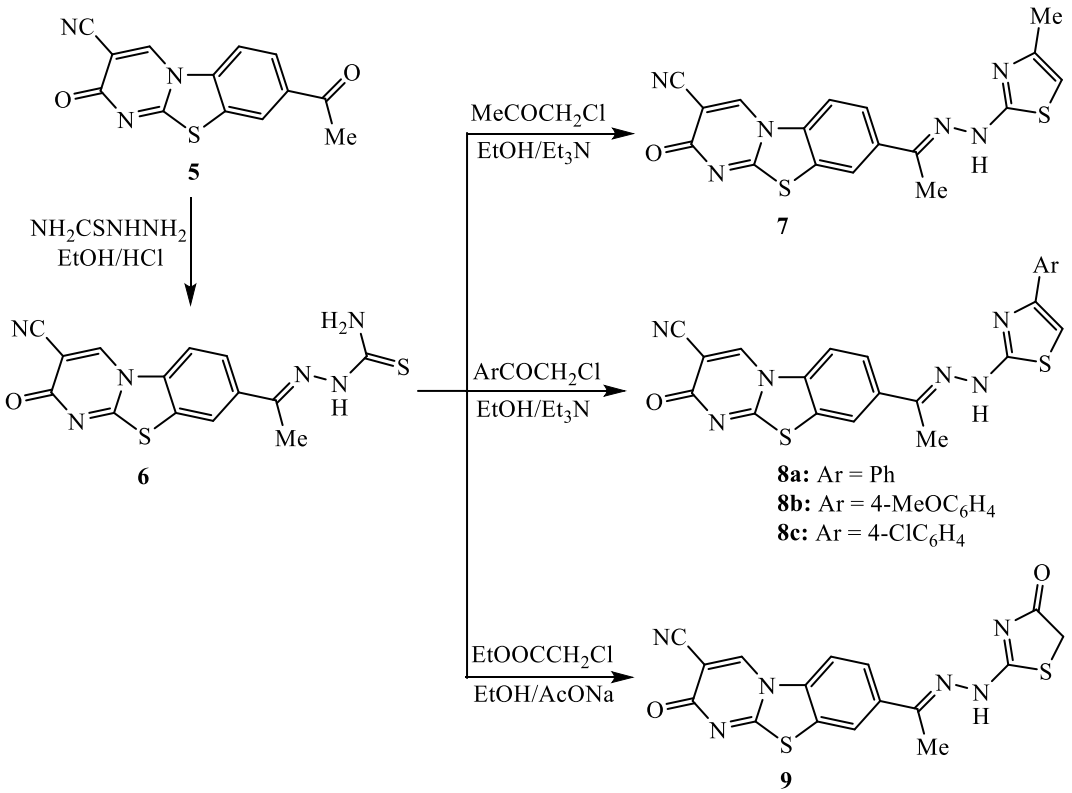

Scheme 2. Synthesis of benzothiazolo[3,2-*a*]pyrimidine–thiazole conjugates **7, 8**, and **9**.

produce the conforming thiosemicarbazone compound **6** (Scheme 2). The thiosemicarbazone compound **6** was used as a precursor to produce a series of benzothiazolo[3,2-*a*]pyrimidine-thiazole conjugates by reacting with different α-chloroketones and/or α-chloroesters (Hantzsch type reaction). The benzothiazolopyrimidine-thiazole conjugate **7** was synthesized by reacting thiosemicarbazone compound **6** with chloroacetone in ethanol and triethylamine. The three benzothiazolopyrimidine-thiazole conjugates **8a**, **8b**, and **8c**, having phenyl or phenylene group at position-4 of the new thiazole, were produced under the same conditions. These conjugates **8a**, **8b**, and **8c** were obtained by reacting thiosemicarbazone compound **6** with different (un)substituted phenacyl chloride derivatives (namely; phenacyl chloride, 4-methoxyphenacyl chloride, and 4-chlorophenacyl chloride). Moreover, the synthesis of the fifth benzothiazolopyrimidine-thiazole conjugate **9**, which is distinguished by the new thiazolin-4-one skeleton, was achieved by reacting thiosemicarbazone compound **6** with ethyl chloroacetate in refluxing ethanol and sodium acetate.

3.2. Molecular modelling

The DFT optimization of the parent compound **5 (**8-acetyl-3-cyano-2-oxo-2*H*-benzo [4,5]thiazolo[3,2-*a*]pyrimidine) disclosed that it has planar structure and so the thiosemicarbazone conjugate **6** (Fig. 1). However, the methyl and phenyl thiazolyl hybrids (**7** and **8a-c**) afforded distorted configuration in which the hydrazonyl nitrogen has been moved away from the oxo-benzothiazolopyrimidine and thiazolyl planes, e.g., $C^{7}_{(Btp)}$-$C^{8}_{(Btp)}$-$C_{(Hz)}$-$N_{(Hz)}$ = 18.2–19.6° and $N_{(Hz)}$-$NH_{(Hz)}$-$C^{2}_{(Tz)}$-$S^{1}_{(Tz)}$ = 2.0–2.9°, respectively (Fig. 1 and S1). In oxo-dihydrothiazol-2-yl (**9**), the hydrazonyl nitrogen was shifted out by 6.6° and 21.6°, respectively. Additionally, the substituted phenyl thiazolyl hybrids (**8a-c**) revealed another deformation wherein the phenyl was sloped on the thiazolyl nucleus, i.e., $N^{3}_{(Tz)}$-$C^{4}_{(Tz)}$-$C^{1}_{(PhTz)}$-$C^{2}_{(PhTz)}$ = 3.7–6.6°. Also, the conjugate **9** displayed a non-planar configuration of the oxo-thiazolyl ring as its dihedral angles were 1.0–1.4° region (Table S1).

Further, the comparison of DFT structural features (length and angle of bonds) with the X-ray single crystal correspondents of comparable hybrids [56,57] disclosed a reasonable agreement, lengths discrepancy <0.11 Å (RMSD = 0.05) and angles up to 11.0° (RMSD = 3.7–4.30). The dissimilarity could be attributed to an individual molecule in gaseous state was considered in quantum calculations, whereas in solid crystals, molecules suffering columbic interactions [58] (Tables S2–S3).

Since their substantially manipulate the molecule's capability of delivering or receiving electrons [59,60], the HOMO-LUMO's energies and gap, called frontier molecular orbitals (FMO's), has obtained distinct importance. The FMO's graph of the hybrid **5** displayed that its HOMO and LUMO was extend over the complete molecule (π and π*, respectively), whereas, the thiosemicarbazone **6** exhibited completely different composition of the HOMO, localized on the thiosemicarbazone group (non-bonding MO), but the LUMO preserved cover the full molecule (π*-orbital) (Fig. 2). Hence, the HOMO-LUMO charge-transfer (CT) possibly will be denoted as π→π* in **5** and n→π* in **6**. In conformity, the analogs FMO energies revealed that hybrid **6** has lower E_H and E_L than **5**. As well, the

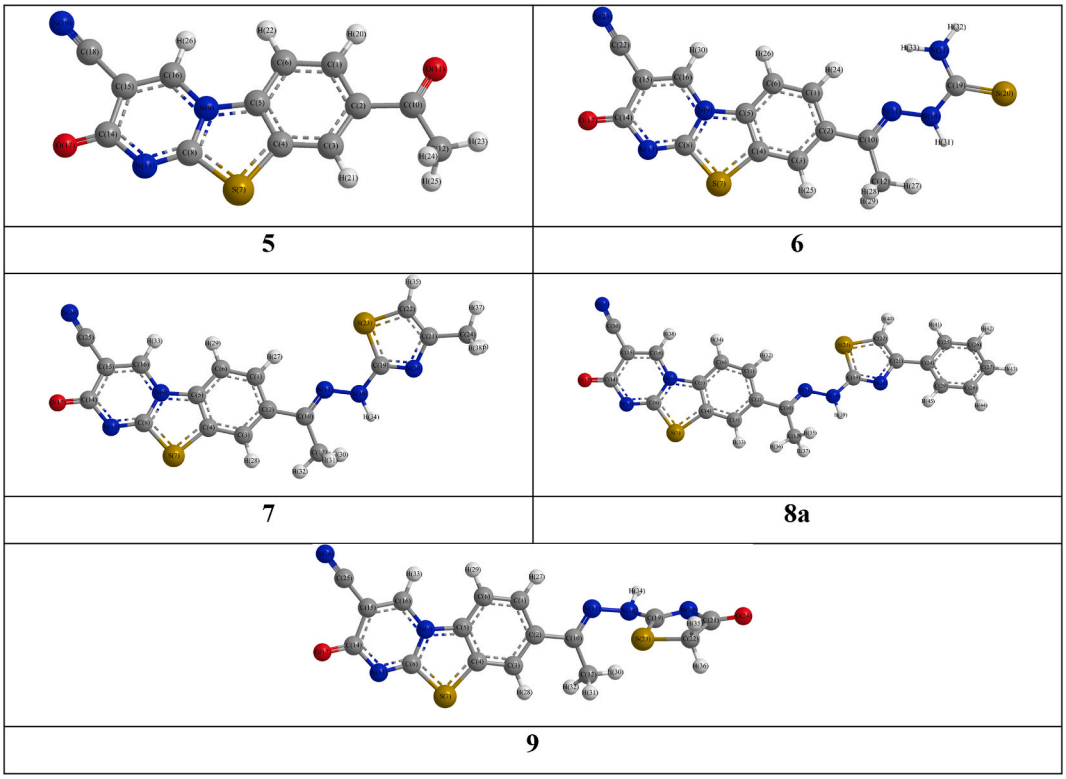

Fig. 1. Compounds **5–7**, **8a** and **9** DFT Optimized structures.

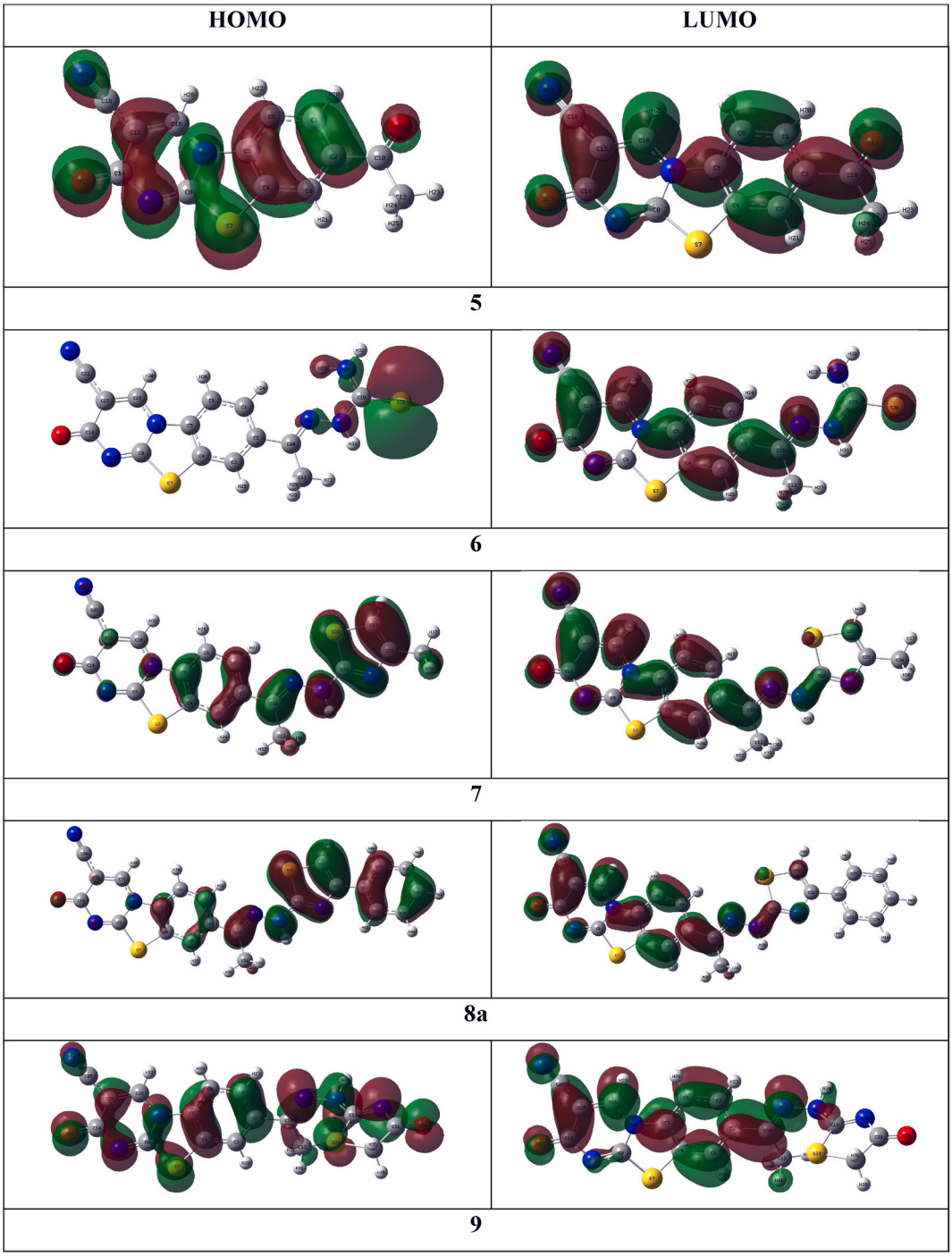

Fig. 2. The FMO-plot for hybrids **5–7**, **8a** and **9**.

thiosemicarbazone **6** has reduced energy gap ($\Delta E_{H\text{-}L}$) than the parent **5**, 3.42 and 4.17 eV, respectively (Table 1). Instead, the substituted thiazoles **7** and **8a-c** plots revealed equivalent configurations in which the HOMO was built mainly from the of the hydrazonylthiazole with partial contribution of the fused tricyclic nuclei. Nevertheless, their LUMO may be denoted as the π*-orbital of the benzothiazolopyrimidine hydrazonyl group (Fig. 2 and S2). Consequently, the conjugates **7** and **8a-c** delivered alike FMO's energies, e.g., the $\Delta E_{H\text{-}L}$ have been ranged from 3.01 to 3.33 eV. Eventually, the oxothiazolyl hybrid **9** possessed similar configuration of the LUMO whereas his HOMO has been fabricated from the π-orbital of the benzothiazolopyrimidine hydrazonyl along with high sharing of the oxothiazole lone pair of electrons. As a result, the researched hybrids delivered FMO's gap ($\Delta E_{H\text{-}L}$) ranged from 3.01 to

Table 1
FMO's energies and reactivity descriptors (eV) of investigated compounds.

Compound	E_H	E_L	ΔE_{H-L}	χ	η	δ	ω	$\omega+$	$\omega-$
5	−7.20	−3.03	4.17	5.12	2.09	0.48	6.28	3.98	9.10
6	−6.33	−2.91	3.42	4.62	1.71	0.58	6.25	4.15	8.77
7	−6.01	−2.67	3.33	4.34	1.67	0.60	5.65	3.69	8.03
8a	−5.93	−2.71	3.22	4.32	1.61	0.62	5.80	3.84	8.16
8b	−5.69	−2.68	3.01	4.19	1.50	0.67	5.83	3.92	8.11
8c	−6.04	−2.77	3.27	4.40	1.64	0.61	5.92	3.93	8.33
9	−7.12	−3.14	3.98	5.13	1.99	0.50	6.60	4.29	9.42

4.17 eV wherein the **8a-c** have the least quantities according the arrangement **8b** < **8a** < **8c** < **7** < **6** < **9** < **5** (Table 1).

Additionally, the chemical reactivity signifiers have been figured by the use of the FMO's energies as shown below [61].

$$\chi = -\frac{1}{2}(E_{HOMO} + E_{LUMO})\eta = -\frac{1}{2}(E_{HOMO} - E_{LUMO})\delta = \frac{1}{\eta}$$

$$\omega = \frac{\chi^2}{8\eta}\omega^- = \frac{(3I + A)^2}{16(I - A)}\omega^+ = \frac{(I + 3A)^2}{16(I - A)}$$

The electronegativity (χ) and hardness (η) unveiled that compound **8b** has the least measures (4.19 and 1.5 eV) although **5** exhibited the minimum softness (δ = 0.48 eV). The electrophilicity index (ω), 5.65–6.60 eV, validated the reputable electrophilicity nature of the conjugates, ω > 1.5 eV [62], and could be organized: **7** < **8a** < **8b** < **8c** < **6** < **5** < **9**. Similarly, the electron donation and acceptance powers (ω^+ and ω^-) pointed to the improved tendency to give than getting electrons [62,63] (Table 1).

The electronegativity and intramolecular charge transfer of the explored hybrids were empathized by investigating their Mulliken's atomic charges [64]. The benzothiazolopyrimidine sulfur ($S^{10}_{(Btp)}$) in all the studied derivatives was positively charged where **3** and **9** displayed higher value than others, 0.223 and 0.212–0.218, respectively. In contrast, its nitrogen atoms ($N^{1}_{(Btp)}$ and $N^{5}_{(Btp)}$) have different negative charge, −0.198 to −0.201 and −0.169 to −0.171, respectively (Table S4). Likewise, the benzothiazolopyrimidine oxo-substituent ($O_{(OxBtp)}$) acquired higher negative charge than nitrogen atom of the cyano-substituent ($NC_{(OxBtp)}$), −0.310 to −0.317 and −0.151 to −0.157, respectively. Furthermore, in thiosemicarbazone **6**, the carbothioamide nitrogen atoms $N_{(Tsc)}$ and $NH_{(Tsc)}$ were negatively charged, −0.185 and −0.330. However, upon cyclization of the carbothioamide to form thiazole ring, the $N_{(Tsc)}$ and $NH_{(Tsc)}$ converted to hydrazonyl atoms, $N_{(Hz)}$ and $NH_{(Hz)}$, and thus, the charge of the former was reduced to ~ −0.138 while the latter slightly increased ~ −0.343. Also, the transformation of the carbothioamide sulfur and nitrogen, $SC_{(Tsc)}$ and $NH_{2(Tsc)}$, that have negative charges, −0.282 and −0.676, into the thiazolyl $S^{1}_{(Tz)}$ and $N^{3}_{(Tz)}$ resulted in inversion of the sulfur to be positively charged (0.155–0.221) and reduction of the nitrogen charge (−0.228 to −0.280) (Table S4).

Moreover, the Fukui's indices were evaluated to discover the nucleophilic (f_k^+) and electrophilic (f_k^-) attacks susceptible sites [65,66]. But, Fukui's indices occasionally disclosed inaccurate estimate of the active sites, hence, the local relative electrophilicity (s_k^-/s_k^+) and nucleophilicity (s_k^+/s_k^-) factors were evaluated and competed with the equivalent Fukui's indices [67]. The electrophilic indices (f_k^-) of the parent **5** presented the oxygen of oxo and acetyl substituents ($O_{(OxBtp)}$ and $OC_{(Act)}$) as the most active atoms. However, the thiosemicarbazone **6** displayed the carbothioamide sulfur and nitrogen ($SC_{(Tsc)}$ and $NH_{2(Tsc)}$) in the primary and subsequent places, respectively. In contrary, the thiazolyl hybrids **7** and **8a-c** unveiled fully distinctive array in which the sulfur and carbon of thiazole ($S^{1}_{(Tz)}$ and $C^{5}_{(Tz)}$) seized the foremost positions, respectively. Similarly, the relative electrophilicity descriptors (s_k^-/s_k^+) evoked comparable organization with those of Fukui's indices in case of derivatives **5** and **6**. While, the thiazolyl hybrids **7** and **8a-c** displayed close patterns but differ from that observed in Fukui's indices wherein the thiazolyl carbon and sulfur ($C^{2}_{(Tz)}$ and $S^{1}_{(Tz)}$) captured the topmost places in **7**, respectively, and appeared after the phenylthiazole carbon ($C^{2}_{(PhTz)}$) in **8a-c** (Table S5). Otherwise, the Fukui's indices (f_k^+) designated the acetyl oxygen ($OC_{(Act)}$) and carbothioamide sulfur ($SC_{(Tsc)}$) as the furthermost active sites in hybrids **5** and **6**, respectively. Although, the nitrogen of the cyano-substituent ($NC_{(Btp)}$) occupied the second place in **5** and **6**, it captured the first position in derivatives **7**, **8a-c** and **9**. Meanwhile, the benzothiazolopyrimidine carbon and sulfur ($C^{4}_{(Btp)}$ and $S^{10}_{(Btp)}$) were appeared in the second and third positions, respectively, in conjugates **7** and **8a-c**. Alternatively, the relative nucleophilicity descriptors (s_k^+/s_k^-) evoked another fashions of the highly liable atoms. For example, the phenylthiazoles **8a-c** in addition to **6** and **9** presented the benzothiazolopyrimidine carbon ($C^{8}_{(Btp)}$) on top position followed by the $C^{4}_{(Btp)}$. However, the derivative **7** showed these carbons in reversed order (Table S5).

To illuminate electronic density distribution and softness, which mainly affect the intermolecular interactions [68], the molecular polarizability (α_{total}), hyperpolarizabilities (β_{total}), and dipole moment (μ), of the conjugates were figured [69].

$$\mu = \left(\mu_x^2 + \mu_y^2 + \mu_z^2\right)\alpha_{total} = \frac{(\alpha_{xx} + \alpha_{yy} + \alpha_{zz})}{3}$$

$$\beta_{total} = \sqrt{\left(\beta_{xxx} + \beta_{xyy} + \beta_{xzz}\right)^2 + \left(\beta_{yyy} + \beta_{yzz} + \beta_{yxx}\right)^2 + \left(\beta_{zzz} + \beta_{zxx} + \beta_{zyy}\right)^2}$$

The hybrids displayed widespread dipole moment (μ) fluctuated from 5.22 D for **9** to 12.72 D for **8b**, which superior than urea,

reference substance [70], 3.80–9.26 folds (Table 2). Also, the polarizability unveiled that the parent **5** showed the minimum value but the phenylthiazole **8c** had the greatest, $\alpha_{total} = 2.01$ and 3.84×10^{-23} esu, respectively. As well, the first-order hyperpolarizability denoted hybrid **5** as the least, $\beta_{total} = 3.04 \times 10^{-30}$ esu, and the conjugate **8b** as the most, $\beta_{total} = 18.80 \times 10^{-30}$ esu. Compared to urea [70], the entire hybrids owned superior hyperpolarizability, 8.14–50.35 folds, and could be organized as **5** < **6** < **9** < **7** < **8c** < **8a** < **8b** (Table 2).

3.3. Antimicrobial activity

The antimicrobial activity outcomes are presented in Table 3. Derivative **5** in general showed the lowest antimicrobial inhibitions across all tested pathogens in comparison to the applied references (Chloramphenicol, Cephalothin, and Cycloheximide), and the proper inhibition towards *C. albicans* (MIC <213 μg/mL). However, derivative **6** established a coherent range of inhibition with MIC values near those of derivative **5**, outstandingly appropriate against *E. coli* and *C. albicans* over MIC <44 and < 210 μg/mL, individually. The similar performance across both Gram (+ve) and Gram (-ve) bacteria indicates a balanced antimicrobial capability, that could be advantageous for treating infections caused by multiple types of bacteria. Though, derivative **7** displayed significant inhibition against most of the examined pathogens, most noted efficiency towards *E. coli* (MIC <41 μg/mL) and promising inhibition towards *S. aureus* (MIC <39 μg/mL) as (-ve) Gram bacterial stains in addition to weak efficiency towards *C. albicans* (fungi) (MIC <241 μg/mL). Moreover, derivative **8a** was particularly effective against *E. coli* (MIC <36 μg/mL), showed significant inhibition towards *S. typhimurium* (MIC <129 μg/mL). However, its worst inhibition towards *C. albicans* was higher (MIC <238 μg/mL), indicating a decreased antifungal inhibition. But, derivative **8b** revealed promising values of MIC towards *S. aureus* and *B. subtilis* such as (+ve) Gram strain through (MIC <40 and < 47 μg/mL, respectively). Likewise, **8b** discovered good inhibition towards *E. coli* (-ve Gram bacteria) through (MIC <39 μg/mL), suggesting a potential preference or enhanced effectiveness against these pathogens. Interestingly, it also showed the highest MIC value (<192 μg/mL) against *C. albicans* (fungi), leading to a auspicious applicant for further development against both bacterial and fungal infections. Moreover, derivative **8c** demonstrated superior inhibition, mainly towards both (Gram + ve) and (Gram -ve) strains, through the highest effectiveness (MIC <35 μg/mL towards *S. aureus*), (MIC <29 μg/mL towards *E. coli*), respectively. This suggests a strong interaction with and disruption of bacterial membranes or essential pathways. Additionally, its good MIC against *C. albicans* (MIC <207 μg/mL), while not the lowest, is competitive, indicating broad-spectrum potential. Further, derivative **9** presented consistent antimicrobial inhibition against most bacterial strains and weak inhibition against antifungal strain (MIC <218 μg/mL against *C. albicans*). This consistent activity profile suggests that derivative **9** may have an effective action that adopts a common target present in both (Gram + ve) and (Gram -ve) strains.

3.4. Structural activity relationship (SAR)

Based on the antimicrobial activity of seven benzothiazolo[3,2-a]pyrimidine clubbed thiazole derivatives, they were assigned toward a panel of pathogens, comprising Gram + ve and Gram -ve (bacteria) and *C. albicans* (fungi). The results were associated with standard antimicrobials, including chloramphenicol, cephalothin (bacteria), and cycloheximide (fungi), to evaluate their relative effectiveness. Derivatives **5** that contain the acetyl group at the 8-position in addition to the nitrile group at the 3-position may contribute to the solubility of bacterial cell walls, interacting with specific targets within microbial cells, enhancing slight antimicrobial inhibition in comparison to the rest of the derivatives. However, derivative **6** with the ethylidene hydrazine carbothioamide moiety may subsidize to interacting and participating in microbial proteins, with slightly improved inhibition against the other microbes too. Meanwhile, derivative **7**, which has a methyl group on the thiazolyl ring, may enhance lipophilicity and improve cellular uptake. The presence of the hydrazineylidene moiety may also simplify interactions with bacterial proteins, demonstrating effective inhibition against *S. aureus*, moderate inhibition against other bacteria, and slight inhibition against fungi. Also, derivatives **8a–c** have substitutions on the phenyl ring that modify the molecule's overall hydrophobic and electronic character. Derivative **8c** which substituted by *p*-chlorine atom that makes it more effective, most likely by improving its interactions with microbial receptors that lead to a wider range of activity and the best inhibition against *E. coli*. Furthermore, derivative **9** with a dihydrothiazolyl ring might stabilize the molecule, enhance microbial cell penetration, or interrupt the microbial progressions. It also displayed strong bacterial inhibition, particularly against *E. coli*.

Ultimately, the OriginPro's Multiple Linear Regression procedure (MLR) [71,72] was employed in correlating the antimicrobial effectiveness (MIC), as dependent variable, with the quantum chemical calculation parameters, as independent variables (Table 4). The data designated that the FMO's gap and softness have the utmost influence as both showed exponential coefficients (10^3) with

Table 2
The dipole moment (μ), polarizability (α_{total}), polarizability anisotropy (Δα) and first-order hyperpolarizability (β_{total}) of explored hybrids.

Compound	μ (Debye)	μ/μ_{urea}	α_{total} (esu × 10^{-23})	Δα (esu × 10^{-23})	β_{total} (esu × 10^{-30})	$\beta_{total}/\beta_{urea}$
5	8.69	6.33	2.01	0.62	3.04	8.14
6	6.90	5.02	2.78	1.42	3.05	8.17
7	11.89	8.66	2.86	1.05	9.25	24.73
8a	11.32	8.25	3.42	1.47	13.60	36.29
8b	12.72	9.26	3.61	1.42	18.80	50.35
8c	9.09	6.62	3.84	2.04	12.50	33.30
9	5.22	3.80	3.15	1.65	3.35	8.97

Table 3
The MIC results of the synthesized benzothiazolo[3,2-a]pyrimidine clubbed thiazole derivatives.

Derivative	MIC (μg/mL)				
	Gram + ve Bacteria		Gram -ve Bacteria		Fungi
	S. aureus	B. subtilis	E. coli	S. typhimurium	C. albicans
5	<54	<66	<49	<153	<213
6	<57	<59	<44	<137	<210
7	<39	<61	<41	<145	<241
8a	<50	<68	<36	<129	<238
8b	<40	<47	<39	<141	<192
8c	<35	<72	<29	<132	<207
9	<48	<64	<33	<148	<218
Chloramphenicol	<41	<52	–	–	–
Cephalothin	–	–	<32	<127	–
Cycloheximide	–	–	–	–	<201

Table 4
The MLR coefficient of quantum chemical descriptors.

Microbe	*S. aureus*	*B. subtilis*	*E. coli*	*S. typhimurium*	*C. albicans*
Intercept ($\times 10^2$)	15.8	1.32	9.18	0.23	32.00
E_H ($\times 10^2$)	31.10	−0.44	16.70	−1.61	−1.13
E_L ($\times 10^2$)	−0.16	−21.20	9.49	21.20	3.82
$\Delta E_{H\text{-}L}$ ($\times 10^3$)	1.38	1.11	0.28	1.65	1.77
χ ($\times 10^3$)	3.07	−2.23	2.58	2.02	−4.26
δ ($\times 10^2$)	−13.30	−6.79	−7.34	−9.38	−23.40
R^2	0.9944	0.9615	0.9846	0.9136	0.9367
SD	1.51	2.74	5.62	6.23	17.18

opposite signs implying to activity increases with increasing the energy gap (positive sign) whereas the increase in softness will reduce activity (negative sign). Also, a good regression coefficients and standard deviation values were observed (R^2 = 0.9136–0.9944; SD = 1.51–17.18).

3.5. *DNA gyrase*

Concerning the assessment of DNA *gyrase* inhibition, a decisive enzyme in bacterial DNA replication, the results were documented in Table S6 and Fig. 3. Derivative **5** exhibited reasonable effectiveness against DNA *gyrase* inhibition (IC_{50} = 3.17 ± 0.19 μM), but was less effective compared to the rest of the derivatives. However, derivative **6** demonstrated improved effectiveness (IC_{50} = 2.62 ± 0.43 μM) and proposed a slight effectiveness compared to derivative **5**. Even though derivative **7** showed a slightly lower *gyrase* inhibition (IC_{50} = 2.83 ± 0.26 μM) than derivative **6**, this shows how important substituents are in *gyrase* inhibition. Meanwhile, derivatives **8a–c** exhibited the most potent inhibition amongst the established derivatives. Whereas derivative **8b** showed more potent inhibition (IC_{50} = 1.09 ± 0.32 μM) than ciprofloxacin, signifying a highly effective structural framework for targeting DNA *gyrase*. While derivatives **8a** and **8c** demonstrated strong inhibition, which attentively contends with ciprofloxacin, these outcomes underscore the potential of this type of aryl-thiazole derivative for DNA *gyrase* inhibition. Moreover, derivative **9** exhibited a promising inhibition (IC_{50} = 1.88 ± 0.41 μM), while Cipro. (control) exhibited an inhibition (IC_{50} of 1.47 ± 0.19 μM).

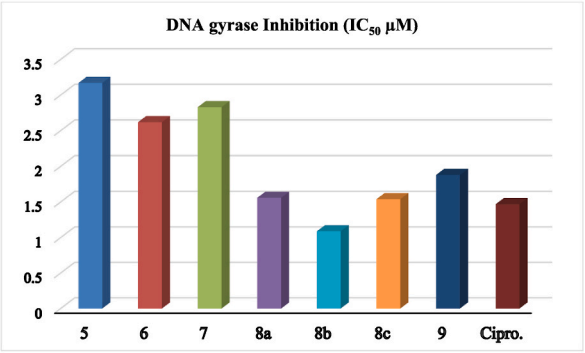

Fig. 3. DNA *gyrase* Inhibition of the prepared benzothiazolo[3,2-a]pyrimidine clubbed thiazole derivatives.

3.6. Molecular docking

By applying the docking inspiration using the M.O.E. 2019 program to the DNA *gyrase* complex represented by (PDB:2XCT) achieved from the Protein Data Bank (Table S7), derivative **5** exhibited a lower score (S = -5.6904 kcal/mol) alongside involving both H-acceptor plus H-π interactions, principally with 2XCT residues Met1113, Lys1270, and Trp592. The molecular distances were realized from 3.11 to 4.06 Å, reflecting drop-binding values (Fig. S3). Meanwhile, derivative **6** disclosed a gradually increasing binding score with S = −6.5810 kcal/mol, enabled *via* both H-donor and acceptor bonds with Asn1109, Gly1111, and Phe1110, with distances between 3.08 and 4.06 Å, suggesting slightly improved binding affinity associated with derivative **5** (Fig. S3).

However, derivative **7** displayed an upright score (S = −6.9850 kcal/mol) among H-acceptor along with π-H bonds with Asn1109, Phe1110, and Leu1298, over which bond distances fluctuated between 3.33 and 4.66 Å, indicating strong and various binding modes of interactions (Fig. S3). Moreover, derivatives **8a-c** demonstrated gradually stronger binding scores (S = −7.1324, −7.6561, and −7.2655 kcal/mol), respectively. These derivatives involved H-donor, H-acceptor, and π-H interactions through particularly prominent bindings including Asp1114, Asp1096, Ser449, and Leu1298 of amino acids in 2XCT, and intermolecular distances were well within the effective range of 3.15–4.63 Å (Fig. 4).

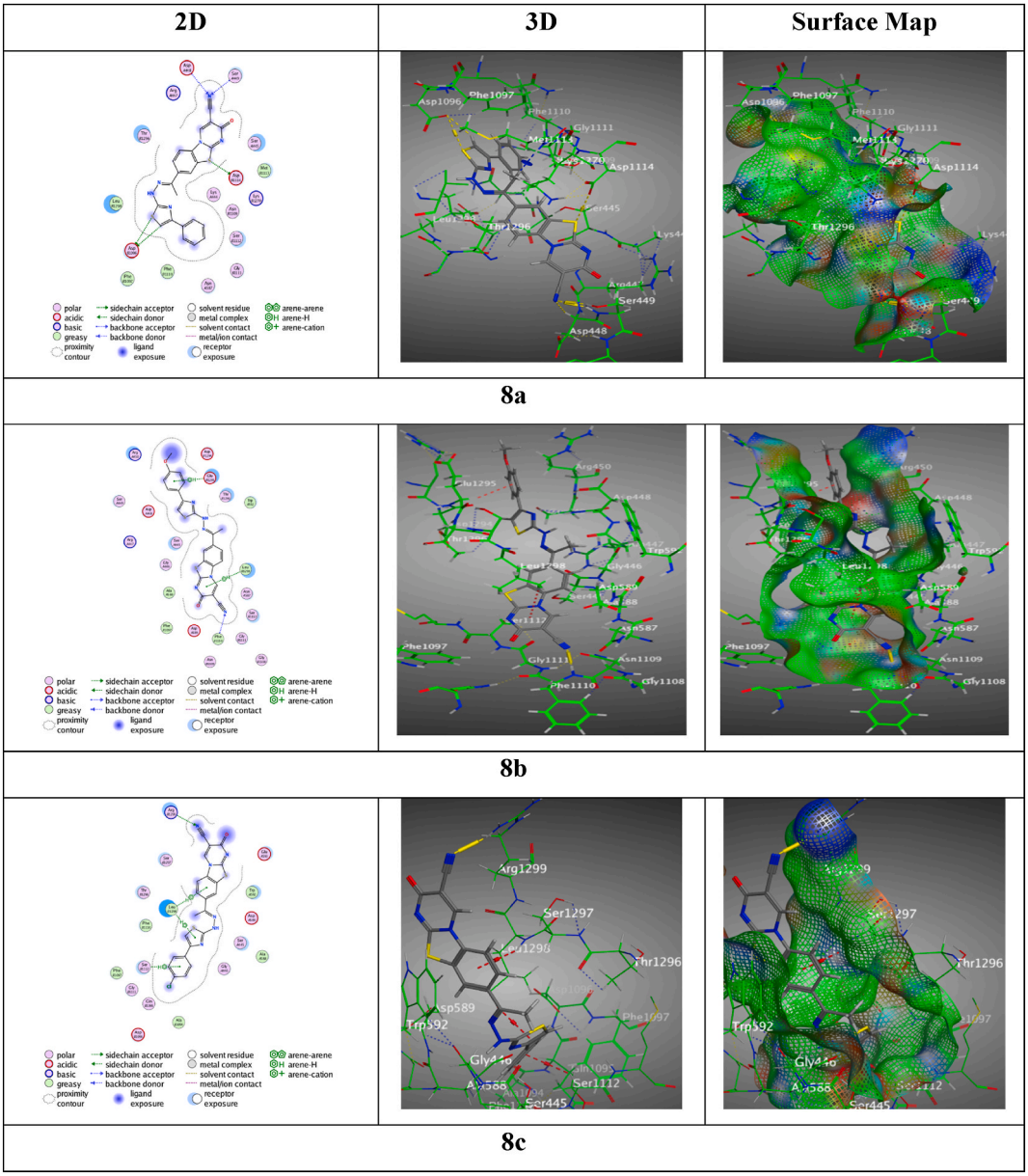

Fig. 4. Docking imaginings of derivatives **8a-c** with 2XCT.

Besides, derivative **9** recorded a proper score (S = −6.9761 kcal/mol), interrelating over H-acceptor besides π-H bonds with amino-acids such as Ser 449, Ala 588, and Thr 1296, with interaction distances signifying vigorous binding affinities (Fig. S3). Furthermore, Cipro. (a drug control) shown a score (S = −6.3210 kcal/mol) over only the H-acceptor bond with Ala588, representing reasonable effectiveness with an intermolecular distance of 3.07 Å (Fig. S3).

3.7. SwissADME

The pharmacokinetic profile and prophesied bioavailability of the studied conjugates were deliberated (Table S8 and Fig. S4). Derivative **5** had a proper M. Wt. = 269.28, demonstrating its lipophilicity with Log Po/w = 1.45 and TPSA = 103.47, indicating that the GI tract would absorb it well. Despite this profile, derivative **5** failed to cross the BBB or a Pgp substrate, indicating its potential for use in peripheral areas. Meanwhile, it showed a bioavailability value = 0.55 besides obeyed Lipinski's rules of drug-likeness. Moreover, derivative **6** exhibited a different profile through M. Wt. = 342.4 over a slightly higher lipophilicity = 1.82. It has a TPSA of 168.9, which contrasts with derivative 5 by indicating lower GI absorption. Furthermore, derivative **6** didn't pass the BBB and showed a peripheral pharmacological application similar to derivative **5**. Moving on to derivatives **7** and **8a-c**, there was an obvious increase in both M. Wt. and lipophilicity, ranging from 380.45 to 476.96 and 2.38 to 3.07, respectively. These derivatives had lower GI absorption and were also not BBB-permeable. Their TPSA displayed a narrow range from 151.92 to 161.15 and emphasized their appropriateness for peripheral uses. Also, these derivatives followed Lipinski's rules, which meant that even though they were bulkier and more lipophilic, they were still considered possible drug candidates on non-CNS boards. Finally, derivative **9** presented an exceptional pharmacokinetic profile at low M. Wt. = 382.42 associated with both derivative **7** and derivatives **8a–c**, through lipophilicity = 1.57, despite having a high TPSA = 165.52, which mostly predicted poor GI absorption, didn't permeate the BBB, and showed no violations of Lipinski's rules. Finally, among the benzothiazole-thiazole conjugates tested, derivative 5 had the lowest projected toxicity. Derivative 5 has the lowest molecular weight (269.28), moderate lipophilicity (Log Po/w = 1.45), good GI absorption, and follows Lipinski's rules, making it a promising candidate for peripheral therapeutic applications that do not cross the blood-brain barrier.

4. Conclusion

The synthetic approach for the production of benzothiazolopyrimidine-thiazole conjugates was started by the reaction of 2-acetamido-6-(2-cyanoacetyl)benzothiazole (**3**) with DMF-DMA followed by cyclization of the produced enamine compound **4** to obtain the 8-acetyl benzothiazolopyrimidine compound **5**. Condensation of compound **5** with thio-semicarbazide afforded the equivalent thio-semicarbazone **6**, which undergoes cyclization upon treatment with chloro-propanone, chloro-acetophenone, and/or ethyl chloroacetate to furnish the benzothiazolopyrimidine-thiazole analogs **7**, **8**, and **9**, individually. The HOMO-LUMO plots indicated that the phenylthiazole hybrids **8a-c** exhibited equivalent configurations and so presented comparable FMO's energy gap where the derivative **8b** has the minimum. Likewise, the first-order hyperpolarizability nominated that analogue **5** demonstrated the least whereas **8b** showed the maximum. The antimicrobial activity indicated that derivative **8c** was the greatest potent towards Gram-negative *E. coli* bacteria (MIC <29 μg/mL), and displayed broad-spectrum antifungal activity (*C. albicans* MIC <207 μg/mL). Meanwhile, hybrid **8b** demonstrated selective efficacy towards Gram (+ve) *S. aureus* and *B. subtilis* strain (MIC <40 and < 47 μg/mL, respectively). On the other hand, the analogs **8a-c** inhibit DNA gyrase more effectively than ciprofloxacin, especially derivative **8b** ($IC_{50} = 1.09 \pm 0.32$ μM). Also, the molecular docking stimulation revealed that both of **8b** and **8a** exhibited the most potent binding affinities (S = −7.6561 and −7.1324 kcal/mol, respectively), characterized by various binding types and strong amino-acid appointments. Thus, the beforementioned results cleared out that such derivatives are promising candidates for further pharmacological and pharmacokinetic development. Likewise, the SwissADME study showed that derivative **5** has significant differences in M.Wt., lipophilicity, and TPSA, that alters its absorption and distribution pathways. The derivative demonstrated high GI absorption and good bioavailability, making it a auspicious applicant for more advance.

Data availability statement

All applicable data are inside the document and presented from the consistent author upon request.

Consent to participate

All authors contributed in a straight line in the present research study.

Consent to publish

CRediT authorship contribution statement

Arwa Alharbi: Writing – original draft, Visualization, Software, Methodology. **Adel I. Alalawy:** Writing – original draft, Visualization, Methodology, Formal analysis. **Shaker T. Alsharif:** Writing – original draft, Visualization, Methodology. **Alaa M. Alqahtani:** Writing – original draft, Visualization, Software. **Ali H. Alessa:** Writing – review & editing, Writing – original draft, Software,

Methodology, Formal analysis. **Mansoor Alsahag:** Writing – review & editing, Writing – original draft, Software, Methodology. **Ali Alisaac:** Writing – original draft, Visualization, Investigation, Formal analysis. **Nashwa M. El-Metwaly:** Writing – review & editing, Supervision, Project administration.

Declaration of competing interest

The authors declare that they have no known competing financial interests or personal relationships that could have appeared to influence the work reported in this paper.

Appendix ASupplementary data

Supplementary data to this article can be found online at https://doi.org/10.1016/j.heliyon.2024.e38905.

References

[1] M.A. Salam, M.Y. Al-Amin, M.T. Salam, J.S. Pawar, N. Akhter, A.A. Rabaan, M.A.A. Alqumber, Antimicrobial resistance: a growing serious threat for global public health, Healthcare 11 (2023) 1946.
[2] M. Aijaz, M. Ahmad, M.A. Ansari, S. Ahmad, Antimicrobial resistance in a globalized world: current challenges and future perspectives, International Journal of Pharmaceutical Drug Design 1 (2023) 7.
[3] S.K. Ahmed, S. Hussein, K. Qurbani, R.H. Ibrahim, A. Fareeq, K.A. Mahmood, M.G. Mohamed, Antimicrobial resistance: impacts, challenges, and future prospects, Journal of Medicine, Surgery, and Public Health 2 (2024) 100081.
[4] K.W.K. Tang, B.C. Millar, J.E. Moore, Antimicrobial resistance (AMR), Br. J. Biomed. Sci. 80 (2023) 11387.
[5] M.E. Velazquez-Meza, M. Galarde-López, B. Carrillo-Quiróz, C.M. Alpuche-Aranda, Antimicrobial resistance: one health approach, Vet. World 15 (2022) 743.
[6] M. Saha, A. Sarkar, Review on multiple facets of drug resistance: a rising challenge in the 21st century, Journal of Xenobiotics 11 (2021) 197.
[7] G. Muteeb, M.T. Rehman, M. Shahwan, M. Aatif, Origin of antibiotics and antibiotic resistance, and their impacts on drug development: a narrative review, Pharmaceuticals 16 (2023) 1615.
[8] Y.K. Schneider, Bacterial natural product drug discovery for new antibiotics: strategies for tackling the problem of antibiotic resistance by efficient bioprospecting, Antibiotics 10 (2021) 842.
[9] M. Terreni, M. Taccani, M. Pregnolato, New antibiotics for multidrug-resistant bacterial strains: latest research developments and future perspectives, Molecules 26 (2021) 2671.
[10] N. Poonia, K. Lal, A. Kumar, A. Kumar, S. Sahu, A.T.K. Baidya, R. Kumar, Urea-thiazole/benzothiazole hybrids with a triazole linker: synthesis, antimicrobial potential, pharmacokinetic profile and in silico mechanistic studies, Mol. Divers. 26 (2022) 2375.
[11] A. Petrou, M. Fesatidou, A. Geronikaki, Thiazole ring—a biologically active scaffold, Molecules 26 (2021) 3166.
[12] A. Kamal, M.A.H. Syed, S.M. Mohammed, Therapeutic potential of benzothiazoles: a patent review (2010–2014), Expert Opin. Ther. Pat. 25 (2015) 335.
[13] S. Agarwal, D. Gandhi, P. Kalal, Benzothiazole: a versatile and multitargeted pharmacophore in the field of medicinal chemistry, Lett. Org. Chem. 14 (2017) 729.
[14] P.C. Sharma, D. Sharma, A. Sharma, K.K. Bansal, H. Rajak, S. Sharma, V.K. Thakur, New horizons in benzothiazole scaffold for cancer therapy: advances in bioactivity, functionality, and chemistry, Appl. Mater. Today 20 (2020) 100783.
[15] M. Bhat, S.L. Belagali, Structural activity relationship and importance of benzothiazole derivatives in medicinal chemistry: a comprehensive review, Mini Rev. Org. Chem. 17 (2020) 323.
[16] E.N. Djuidje, S. Sciabica, R. Buzzi, V. Dissette, J. Balzarini, S. Liekens, E. Serra, E. Andreotti, S. Manfredini, S. Vertuani, Design, synthesis and evaluation of benzothiazole derivatives as multifunctional agents, Bioorg. Chem. 101 (2020) 103960.
[17] R.K. Yadav, R. Kumar, H. Singh, A. Mazumdar, B. Chauhan, M. Abdullah, Recent insights on synthetic methods and pharmacological potential in relation with structure of benzothiazoles, Med. Chem. 19 (2023) 325.
[18] M. Gjorgjieva, T. Tomašič, D. Kikelj, L.P. Mašič, Benzothiazole-based compounds in antibacterial drug discovery, Curr. Med. Chem. 25 (2018) 5218.
[19] S. Cascioferro, B. Parrino, D. Carbone, D. Schillaci, E. Giovannetti, G. Cirrincione, P. Diana, Thiazoles, their benzofused systems, and thiazolidinone derivatives: versatile and promising tools to combat antibiotic resistance, J. Med. Chem. 63 (2020) 7923.
[20] G.S. Shetye, S.G. Franzblau, S. Cho, New tuberculosis drug targets, their inhibitors, and potential therapeutic impact, Transl. Res. 220 (2020) 68.
[21] K.P. Yadav, M.A. Rahman, S. Nishad, S.K. Maurya, M. Anas, M. Mujahid, Synthesis and biological activities of benzothiazole derivatives: a review, Intelligent Pharmacy 1 (2023) 122.
[22] C.G.L. Veale, Unpacking the Pathogen Box—an open source tool for fighting neglected tropical disease, ChemMedChem 14 (2019) 386.
[23] M. Haroun, Review on the developments of benzothiazole-containing antimicrobial agents, Curr. Top. Med. Chem. 22 (2022) 2630.
[24] A. Alsharif, M. Allahyani, A. Aljuaid, A.A. Alsaiari, M.M. Almehmadi, M. Asif, Diverse pharmacological potential of various substituted pyrimidine derivatives, Curr. Org. Chem. 27 (2023) 1779.
[25] B. Nammalwar, R.A. Bunce, Recent advances in pyrimidine-based drugs, Pharmaceuticals 17 (2024) 104.
[26] B. Lippert, P.J. Sanz Miguel, The renaissance of metal–pyrimidine nucleobase coordination chemistry, Acc. Chem. Res. 49 (2016) 1537.
[27] F. Bu, X. Qin, T. Wang, N. Li, M. Zheng, Z. Wu, K. Ma, Unlocking potential biomarkers bridging coronary atherosclerosis and pyrimidine metabolism-associated genes through an integrated bioinformatics and machine learning approach, BMC Cardiovasc. Disord. 24 (2024) 148.
[28] W. Wang, J. Cui, H. Ma, W. Lu, J. Huang, Targeting pyrimidine metabolism in the era of precision cancer medicine, Front. oncol. 11 (2021) 684961.
[29] S. Kumar, A. Deep, B. Narasimhan, A review on synthesis, anticancer and antiviral potentials of pyrimidine derivatives, Curr. Bioact. Compd. 15 (2019) 289.
[30] A.U. Nerkar, Use of pyrimidine and its derivative in pharmaceuticals: a review, J. Advan. Chem. Sci. (2021) 729.
[31] J. Basha, N.M. Goudgaon, A comprehensive review on pyrimidine analogs-versatile scaffold with medicinal and biological potential, J. Mol. Struct. 1246 (2021) 131168.
[32] S. Mohana Roopan, R. Sompalle, Synthetic chemistry of pyrimidines and fused pyrimidines: a review, Synth. Commun. 46 (2016) 645–672.
[33] A. K Keshari, A.K. Singh, S. Saha, Bridgehead nitrogen thiazolo[3,2-*a*]pyrimidine: a privileged structural framework in drug discovery, Mini Rev. Med. Chem. 17 (2017) 1488.
[34] O. Alam, N. Shrivastava, P. Alam, Pyrimidine candidate as promising scaffold and their biological evaluation, International Journal of Pharmacology and Pharmaceutical Sciences 2 (2015) 55.
[35] N.B. Patel, A.C. Purohit, D. Rajani, Newer thiazolopyrimidine-based sulfonamides clubbed with benzothiazole moiety: synthesis and biological evaluation, Med. Chem. Res. 23 (2014) 4789.
[36] M. Jadhav, K. Sankhe, R.R. Bhandare, Z. Edis, S.H. Bloukh, T.A. Khan, Synthetic strategies of pyrimidine-based scaffolds as aurora kinase and polo-like kinase inhibitors, Molecules 26 (2021) 5170.

[37] A.M. Saleh, H.A. Mahdy, M.A. El-Zahabi, A.B.M. Mehany, M.M. Khalifa, I.H. Eissa, Design, synthesis, in silico studies, and biological evaluation of novel pyrimidine-5-carbonitrile derivatives as potential anti-proliferative agents, VEGFR-2 inhibitors and apoptotic inducers, RSC Adv. 13 (2023) 22122.
[38] E.A. Alodeani, M.A. Izhari, M. Arshad, Pharmacological potential and medicinal significance of versatile pyrimidine nucleus, EJBPS 1 (2014) 504.
[39] E. Zarenezhad, M. Farjam, A. Iraji, Synthesis and biological activity of pyrimidines-containing hybrids: focusing on pharmacological application, J. Mol. Struct. 1230 (2021) 129833.
[40] C.M. Bandaru, N. Poojith, S.S. Jadav, M.V. Basaveswara Rao, K.S. Babu, R. Sreenivasulu, R. Alluri, Design, synthesis, anticancer evaluation, and molecular docking studies of thiazole–pyrimidine linked amide derivatives, Polycyclic Aromat. Compd. 42 (2022) 5368.
[41] M. Frisch, G. Trucks, H. Schlegel, G. Scuseria, M. Robb, J. Cheeseman, G. Scalmani, V. Barone, B. Mennucci, G. Petersson, Gaussian 09W, Gaussian. Inc., Wallingford, CT, USA, 2009.
[42] A.D. Becke, Density-functional thermochemistry. III. The role of exact exchange, J. Chem. Phys. 98 (1993) 5648.
[43] C. Lee, W. Yang, R.G. Parr, Development of the Colle-Salvetti correlation-energy formula into a functional of the electron density, Phys. Rev. B Condens. Matter 37 (1988) 785.
[44] J.P. Perdew, Y. Wang, Pair-distribution function and its coupling-constant average for the spin-polarized electron gas, Phys. Rev. B Condens. Matter 46 (1992) 12947.
[45] R. Dennington, T. Keith, J. Millam, GaussView, Version 5, Semichem Inc., Shawnee Mission, KS, 2009.
[46] B. Delley, Ground-state enthalpies: evaluation of electronic structure approaches with emphasis on the density functional method, J. Phys. Chem. A 110 (2006) 13632.
[47] D.S. Biovia, Materials Studio, Dassault Systèmes, San Diego, 2017.
[48] N. El-Gohary, M. Shaaban, Synthesis and biological evaluation of a new series of benzimidazole derivatives as antimicrobial, antiquorum-sensing and antitumor agents, Eur. J. Med. Chem. 131 (2017) 255.
[49] A.A. Abd Elhameed, N.S. El-Gohary, E.R. El-Bendary, M.I. Shaaban, S.M. Bayomi, Synthesis and biological screening of new thiazolo[4,5-*d*]pyrimidine and dithiazolo[3,2-*a*: 5′,4′-*e*]pyrimidinone derivatives as antimicrobial, antiquorum-sensing and antitumor agents, Bioorg. Chem. 81 (2018) 299.
[50] N.A. Alhakamy, A.O. Noor, K.M. Hosny, J.J. Nasr, M.M. Fouda, T.A. Khattab, H.E. Gaffer, Synthesis of new cyanopyridine scaffolds and their biological activities, Curr. Org. Synth. 17 (2020) 567.
[51] N.A. Alenazi, H. Alharbi, A.F. Qarah, A. Alsoliemy, M.M. Abualnaja, A. Karkashan, B. Abbas, N.M. El-Metwaly, New thieno[2,3-*b*]pyridine-based compounds: synthesis, molecular modelling, antibacterial and antifungal activities, Arab. J. Chem. 16 (2023) 105226.
[52] H.A. Aziz, A.M.M. El-Saghier, M. Badr, G.E.-D.A. Abuo-Rahma, M.E. Shoman, Thiazolidine-2,4-dione-linked ciprofloxacin derivatives with broad-spectrum antibacterial, MRSA and topoisomerase inhibitory activities, Mol. Divers. 26 (2022) 1743.
[53] R.M. Alqurashi, T.A. Farghaly, R. Sabour, M.R. Shaabana, Design, Synthesis, antimicrobial screening and molecular modeling of novel 6,7-dimethylquinoxalin-2 (1H)-one and thiazole derivatives targeting DNA gyrase enzyme, Bioorg. Chem. 134 (2023) 106433.
[54] N. Nehra, R.K. Tittal, D.G. Vikas, K. Lal, Synthesis, antifungal studies, molecular docking, ADME and DNA interaction studies of 4-hydroxyphenyl benzothiazole linked 1,2,3-triazoles, J. Mol. Struct. 1245 (2021) 131013.
[55] P. Kashyap, S. Verma, P. Gupta, R. Narang, S. Lal, M.J.M.C.R. Devgun, Recent insights into antibacterial potential of benzothiazole derivatives, Med. Chem. Res. 32 (2023) 1543.
[56] A.A. Harutyunyan, G.A. Panosyan, S.G. Chishmarityan, R.A. Tamazyan, A.G. Aivazyan, R.V. Paronikyan, H.M. Stepanyan, R.S. Sukasyan, A.S. Grigoryan, Synthesis and properties of new benzo[4, 5]thiazolo[3, 2-a]pyrimidine derivatives, Russ. J. Org. Chem. 51 (2015) 711.
[57] T. Sankar, S. Naveen, N.K. Lokanath, K. Gunasekaran, Crystal structure of ethyl 4-(2,4-dichlorophenyl)-2-methyl-4H-benzo[4,5]thiazolo[3,2-*a*]pyrimidine-3-carboxylate, Acta Crystallogr. E: Crystallogr. Commun. 71 (2015) o306.
[58] D. Sajan, L. Joseph, N. Vijayan, M. Karabacak, Natural bond orbital analysis, electronic structure, non-linear properties and vibrational spectral analysis of L-histidinium bromide monohydrate: a density functional theory, Spectrochim. Acta Mol. Biomol. Spectrosc. 81 (2011) 85.
[59] M.M. Makhlouf, A.S. Radwan, B. Ghazal, Experimental and DFT insights into molecular structure and optical properties of new chalcones as promising photosensitizers towards solar cell applications, Appl. Surf. Sci. 452 (2018) 337.
[60] A. Bouchoucha, S. Zaater, S. Bouacida, H. Merazig, S. Djabbar, Synthesis and characterization of new complexes of nickel (II), palladium (II) and platinum(II) with derived sulfonamide ligand: structure, DFT study, antibacterial and cytotoxicity activities, J. Mol. Struct. 1161 (2018) 345.
[61] S. Xavier, S. Periandy, S. Ramalingam, NBO, conformational, NLO, HOMO–LUMO, NMR and electronic spectral study on 1-phenyl-1-propanol by quantum computational methods, Spectrochim. Acta Mol. Biomol. Spectrosc. 137 (2015) 306.
[62] S.O. Afolabi, B. Semire, O.K. Akiode, M.A. Idowu, Quantum study on the optoelectronic properties and chemical reactivity of phenoxazine-based organic photosensitizer for solar cell purposes, Theor. Chem. Acc. 141 (2022) 22.
[63] L.R. Domingo, M. Rios-Gutierrez, P. Perez, Applications of the conceptual density functional theory indices to organic chemistry reactivity, Molecules 21 (2016) 748.
[64] J.B. Bhagyasree, H.T. Varghese, C.Y. Panicker, J. Samuel, C. Van Alsenoy, K. Bolelli, I. Yildiz, E. Aki, Vibrational spectroscopic (FT-IR, FT-Raman, ^{1}H NMR and UV) investigations and computational study of 5-nitro-2-(4-nitrobenzyl) benzoxazole, Spectrochim. Acta Mol. Biomol. Spectrosc. 102 (2013) 99.
[65] L.O. Olasunkanmi, I.B. Obot, E.E. Ebenso, Adsorption and corrosion inhibition properties of N-{n-[1-R-5-(quinoxalin-6-yl)-4,5-dihydropyrazol-3-yl]phenyl} methanesulfonamides on mild steel in 1 M HCl: experimental and theoretical studies, RSC Adv. 6 (2016) 86782.
[66] M. Messali, M. Larouj, H. Lgaz, N. Rezki, F. Al-Blewi, M. Aouad, A. Chaouiki, R. Salghi, I.-M. Chung, A new schiff base derivative as an effective corrosion inhibitor for mild steel in acidic media: experimental and computer simulations studies, J. Mol. Struct. 1168 (2018) 39.
[67] R.K. Roy, S. Pal, K. Hirao, On non-negativity of Fukui function indices, J. Chem. Phys. 110 (1999) 8236.
[68] M. Aziz, S.A. Ejaz, N. Tamam, F. Siddique, N. Riaz, F.A. Qais, S. Chtita, J. Iqbal, Identification of potent inhibitors of NEK7 protein using a comprehensive computational approach, Sci. Rep. 12 (2022) 6404.
[69] J.P. Abraham, D. Sajan, I.H. Joe, V.S. Jayakumar, Molecular structure, spectroscopic studies and first-order molecular hyperpolarizabilities of p-amino acetanilide, Spectrochim. Acta Mol. Biomol. Spectrosc. 71 (2008) 355.
[70] A.B. Ahmed, H. Feki, Y. Abid, H. Boughzala, A. Mlayah, Structural, vibrational and theoretical studies of L-histidine bromide, J. Mol. Struct. 888 (2008) 180.
[71] OriginLab, OriginPro OriginLab Corporation Northampton, MA, 2018.
[72] A. Worachartcheewan, C. Nantasenamat, C. Isarankura-Na-Ayudhya, S. Prachayasittikul, V. Prachayasittikul, Predicting the free radical scavenging activity of curcumin derivatives, Chemom. Intell. Lab. Syst. 109 (2011) 207.